

## Mirror Domain Structures Induced by Interlayer Magnetic Wall Coupling

W. S. Lew, S. P. Li, L. Lopez-Diaz, D. C. Hatton, and J. A. C. Bland

*Cavendish Laboratory, University of Cambridge, Madingley Road, Cambridge CB3 0HE, United Kingdom*

(Received 4 February 2002; published 29 May 2003)

We have found that during giant magnetoresistance measurements in  $\sim 10 \times 10 \text{ mm}^2$  NiFe/Cu/Co continuous film spin-valve structures, the resistance value suddenly drops to its absolute minimum during the NiFe reversal. The results reveal that the alignment of all magnetic domains in the NiFe film follow exactly that of corresponding domains in the Co film for an appropriate applied field strength. This phenomenon is caused by trapping of the NiFe domain walls through the magnetostatic interaction with the Co domain-wall stray fields. Consequently, the interlayer domain-wall coupling induces a mirror domain structure in the magnetic trilayer.

DOI: 10.1103/PhysRevLett.90.217201

PACS numbers: 75.60.-d, 75.47.De, 78.20.Ls

Among the most important advances in layered magnetic structures is the discovery of the exchange interaction between ferromagnetic (FM) films across nonmagnetic interlayers. Several types of the interlayer coupling have been studied theoretically and experimentally [1,2]. It was mentioned some 40 years ago that a magnetostatic interaction could arise between the domain-wall stray fields in a FM/N/FM structure, where  $N$  is a nonmagnetic metallic or insulating layer [3,4]. Recently, it was found that repeated switching of the magnetization in the soft layer could decrease the remanent magnetization of the hard magnetic layer in a magnetic tunnel junction structure [5]. To explain this phenomenon, Thomas *et al.* proposed a model of domain-wall induced coupling [6], which provides a good understanding of the observed demagnetizing effect. However, the search continues for an experimental method to detect the wall-wall coupling directly, since the wall-wall coupling is a local effect in the films, and the response of macroscopic quantities to any stimulus could be weak. Recognizing that the stray fields that emanate from the domain walls in both magnetic layers can interact and so influence each other, it suggests that a reasonable approach would be to investigate the pinning effect that is induced by the wall-wall interaction. To probe this pinning effect, one of the magnetic layers in the investigated sample must be magnetically hard and able to provide relatively stable domains; the other magnetic layer must be magnetically soft towards the pinning field which arises from the domain walls in the hard layer. Moreover, high quality films with a small interface roughness [7] and a relatively thick spacer layer are essential to minimize the effect of roughness-induced magnetostatic coupling and interlayer exchange coupling [8]. In this Letter, Ni<sub>80</sub>Fe<sub>20</sub>(60 Å)/Cu(60 Å)/Co(18 Å) spin-valve structures were chosen for the investigation. We have found that during giant magnetoresistance (GMR) measurements, the GMR value has a sudden drop to the absolute minimum value during the process of NiFe reversal, where the resistance due to the parallel magnetization

configuration at saturation is used to calibrate the absolute minimum.

The NiFe/Cu/Co trilayer structures were grown on GaAs(100) substrates using molecular beam epitaxy (MBE) techniques in ultrahigh vacuum conditions ( $2 \times 10^{-10}$  mbar). *In situ* reflection high-energy electron diffraction measurements show that the bottom Co magnetic layer has a bcc structure, whereas the Cu spacer layer and the top NiFe magnetic layer have fcc structures [9,10]. The large 60 Å Cu spacer layer thickness is chosen to minimize the effect of interlayer exchange coupling [11,12]. During GMR measurements, the Co hard layer is first saturated with a high field along the sample global easy axis; the Co magnetization is then partially reversed with a given applied field ( $H_r$ ) in the opposite direction [13]. The domain structures formed in the Co film can be probed by studying the changes of the GMR value, which is sensitive to the relative magnetization orientations in the magnetic layers.

In addition, two spin-valve structures each with step-wedge Co layer thickness were made in separate growth runs in the MBE chamber: Si(001)/Cu(700 Å)/Co(18 Å, 40 Å)/Cu(60 Å)/NiFe(60 Å) and GaAs(100)/Co(30 Å, 40 Å)/Cu(60 Å)/NiFe(60 Å). For the Si substrate system, the Co and NiFe films were grown epitaxially in a fcc structure [13], while the Co films on the GaAs(100) system develop into a combination of bcc and hcp structures with larger thickness [10]. These samples are used as references and the measured results will be used for comparison.

Figure 1 shows the GMR loops obtained for different values of the minimum applied field  $H_r$ . Figure 1(a) is a typical minor GMR loop that corresponds to the magnetization switching of the NiFe soft layer, while the Co magnetization is directed along the global easy axis without any change. The maximum and minimum resistance values correspond to the antiparallel and parallel configurations, respectively. When the size of  $H_r$  is slowly increased, the GMR loops change shape, as shown in Figs. 1(b) and 1(c). The most striking feature in our GMR results is that a significant drop of the resistance

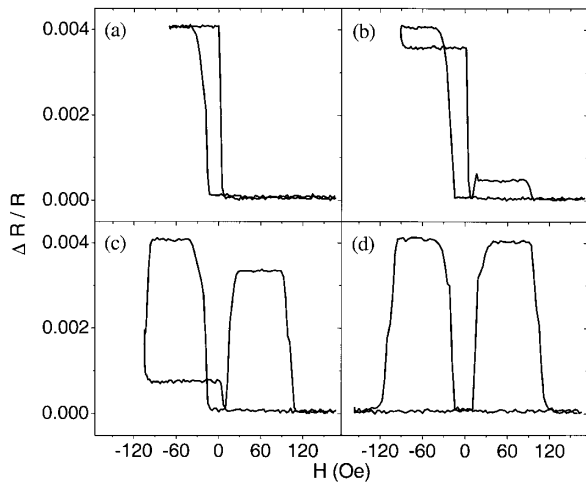


FIG. 1. GMR loops of the NiFe/Cu/Co trilayer structure measured for different values of  $H_r$  (a)  $-70$  Oe, (b)  $-91$  Oe, (c)  $-97$  Oe, (d)  $-156$  Oe. As the value of  $H_r$  is increased, the resistance value drops due to the growing Co domain with a reverse magnetization.

value, to its absolute minimum, has been observed during the reversal of the NiFe layer. This relates to the changes in domain structure and their magnetization directions in the two magnetic layers. We present the  $H_r = -95$  Oe GMR loop, with five schematic magnetization configuration diagrams, in Fig. 2. Starting from point A where the magnetizations of the FM layers are parallel (i), the applied field is then reduced to a negative value at B, whereupon the NiFe magnetization begins to switch and, by the time C is reached, becomes antiparallel to the Co magnetization (ii). As the size of  $H_r$  is slightly larger than the Co nucleation field at D, the magnetization reversal of the Co film is about to begin and a reverse domain evolves. Since the magnetizations in the two magnetic layers are no longer completely antiparallel (iii), the resistance

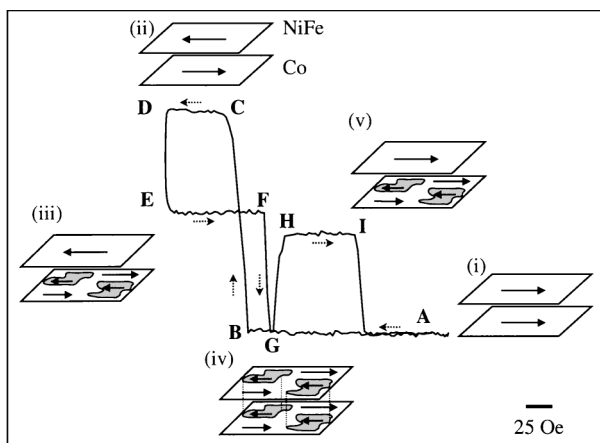


FIG. 2. GMR loop measured with  $H_r = -95$  Oe, along with five schematics of magnetization orientations. The dotted arrows show the sequence of the GMR loop. Mirror domain structures, as shown in schematic (iv), are induced in the trilayer at point G.

value is then reduced with respect to the value at C and D. The resistance value at point E depends on the fraction of the evolved reverse Co layer. Similarly, at F, the NiFe magnetization begins to switch, evolving reverse domains. However, the GMR value suffers a sudden drop to its absolute minimum at point G. The decrease of the GMR value is due to the formation of a unique parallel configuration in the trilayer. The unique configuration is one with Co and NiFe domains with the same magnetization directions, perfectly mirroring each other, as schematically shown in (iv). When the NiFe film fully develops into a single domain state at H, the unique configuration disappears but the magnetizations in both layers are still partially antiparallel to each other (v); therefore, the resistance value is increased. Again, the resistance at point H depends on the fraction of the reversed Co film and this is indicated by the equal values of the resistance changes which correspond to DE and GH on the GMR loop. At point I, the Co magnetization begins to switch back into the single domain state, and the resistance value returns to its absolute minimum in a full parallel configuration. A similar process occurs in the loops in Figs. 1(b) and 1(c), but the different  $H_r$  values give different fractions of reverse Co domains. As long as

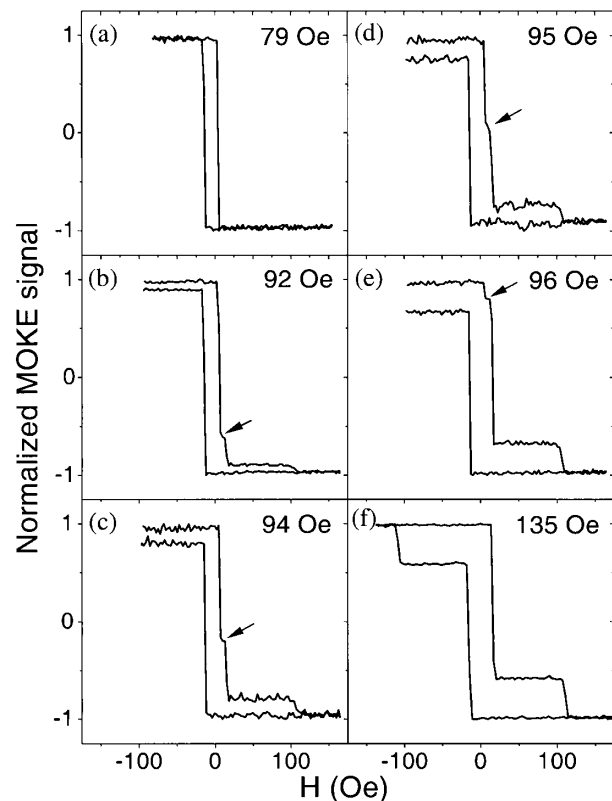


FIG. 3. Measured  $H_r$ -dependent MOKE hysteresis loops. The arrows show the two-step jump which takes place during the reversal of the NiFe magnetization. (a) and (f) have no partial reverse Co domain, hence no two-step jump, where two-step jumps in (b)–(e) indicate the presence of the mirror domain structures.

the reverse Co domain exists, regardless of its fraction, the resistance keeps dropping to its absolute minimum at point *G*. This indicates that the alignment of the reverse NiFe domain follows exactly the profile of the reverse Co domain. When  $H_r$  is larger than the Co switching field, the Co magnetization can be completely reversed instantaneously. Without the reverse Co domain, the mirror domain effect ceases, and a classic full GMR loop is obtained [Fig. 1(d)].

Magneto-optical Kerr effect (MOKE) measurements were also performed to study the magnetization reversal process for various reverse field,  $H_r$ . The obtained MOKE hysteresis loops are shown in Fig. 3. A clear two-step jump can be seen during the switch of the NiFe magnetization [see the arrows in Figs. 3(b)–3(e)]. The two-step jump indicates that, during the reversal of the NiFe magnetization, the NiFe domains with a reverse magnetization are trapped by a pinning field. Complete reversal occurs only after the external field overcomes the pinning field. As the size of  $H_r$  is increased, the second-step jump moves upwards. That shows that the fraction of the reversed NiFe, i.e., the fraction of the NiFe which does not switch until the second step, is becoming larger. A small second-step jump indicates a small reversed fraction in the NiFe, as most of the NiFe moments have switched to the positive direction in the first-step switch, whereas a large second-step jump indicates a large reversed area in the NiFe film, as fewer moments have switched to the positive direction. The two-step jump disappears when there is no more partial reverse magnetization in the Co layer. Moreover, the fractions of reversed area in the two magnetic layers can be expressed by a phenomenological relation  $I_{Co}^p/I_{Co}^i = I_{NiFe}^p/I_{NiFe}^i$ , where  $I_{Co, NiFe}^p$  and  $I_{Co, NiFe}^i$  are the changes in MOKE signal intensity induced by the partial and full switching of Co or NiFe film, respectively. This result is in agreement with the GMR result that the fraction of the reversed NiFe magnetization is the same as that of the Co film.

In the epitaxial Co film the typical magnetic domain size could be as large as  $\sim 100 \mu\text{m}$  [14]; therefore, one can expect that there are numerous magnetic domains mirroring each other in the investigated sample ( $\sim 10 \times 10 \text{mm}^2$ ). We propose that the mirror domain structures inferred from the GMR and MOKE measurements are caused by magnetostatic interactions via domain-wall stray fields from the two FM layers. The pinning field, which traps the NiFe domain wall, in fact originates from the interaction between the stray fields of the Co and NiFe domain walls. In our numerical micromagnetic calculations, Néel

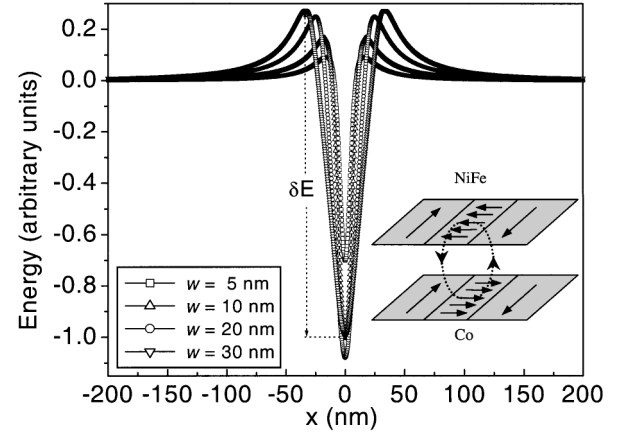


FIG. 4. Calculated interlayer antiparallel domain-wall interaction, with energy in arbitrary units, as a function of wall-wall lateral separation for a NiFe/Cu/Co trilayer with different domain wall thicknesses. The inset shows a schematic for the antiparallel wall-wall interactions.

walls are assumed to be present in the magnetic films [15]. Each wall is considered to be a uniformly magnetized rectangular block of dimensions  $w \times t \times h$ , where  $w$  is the wall width,  $t$  is the layer thickness, and  $h$  is the length of the wall, which is considered to be in the order of the film size and, thus, much larger than the other dimensions. Figure 4 shows the computed values of the magnetostatic interaction energies as a function of the lateral separation  $x$  between the two walls for different  $w$  values. The magnetizations of the two domain walls are in the antiparallel configuration and they are strongly attracted to each other ( $E < 0$ ). However, the position of the walls is less stable when there is a slight offset, and they start to repel each other ( $E > 0$ ) when the offset is high. To escape the pinning the NiFe domain wall must overcome the interaction energy barrier  $\delta E$ . Therefore, to minimize the interaction energy, the NiFe domain wall is pinned exactly on the top of the Co domain wall. Although our additional calculations reveal that the interaction energy barrier  $\delta E$  for antiparallel and parallel pinning is similar, we believe only the antiparallel pinning is present. This is because the reverse domains in both ferromagnetic layers consistently evolve from a saturated magnetization state, and the magnetization of the Néel domain walls in the Co and NiFe layers tend to point in an opposite direction to accommodate the evolving reverse domains.

From Fig. 4, we notice that the pinning energy is very sensitive to the wall parameters, such as the wall width. The magnetostatic interaction between two laterally parallel magnetic walls can be expressed as:

$$F = \mp \frac{2\mu_0 M_1 M_2}{\pi} \int_0^{t_1} \int_0^{t_2} \left( \frac{1}{4(t_0 + \tau_1 + \tau_2)^2 + (w_2 - w_1)^2} - \frac{1}{4(t_0 + \tau_1 + \tau_2)^2 + (w_1 + w_2)^2} \right) d\tau_1 d\tau_2. \quad (1)$$

For an ultrathin magnetic film, the magnitude of the force may be approximated as:

$$F \sim \mp \frac{2\mu_0 M_1 M_2 t_1 t_2}{\pi} \left( \frac{1}{(2t_0 + t_1 + t_2)^2 + (w_2 - w_1)^2} - \frac{1}{(2t_0 + t_1 + t_2)^2 + (w_1 + w_2)^2} \right). \quad (2)$$

The first positive and second negative terms on the right of Eq. (2) correspond to the attractive and repulsive forces, respectively. The symbols  $M_1$  and  $M_2$  are the magnetizations;  $\tau_1$  and  $\tau_2$  are the element thicknesses;  $w_1$  and  $w_2$  are the wall widths;  $t_1$ ,  $t_2$ , and  $t_0$  are the thicknesses of the two magnetic layers and the spacer layer, respectively. From Eq. (2), we can infer that, when the widths of the domain walls in the two magnetic layers are of comparable size ( $w_2 \rightarrow w_1$ ), a strong wall-wall interaction is favored.

To verify this presumption, similar GMR and MOKE measurements were carried out on the Si and GaAs reference samples and the typical results are shown in Fig. 5. Interestingly, the mirror domain effect was repeated in all of the GaAs spin-valve structures, while on the contrary, this effect was not observed in any of the fcc Co spin valves grown on Si. The domain-wall width  $\delta$  is dependent on the material anisotropy  $K$  and the material exchange stiffness  $A$ ,  $\delta \sim \sqrt{A/K}$ . We suppose that, in the fcc Co spin valves, there is no significant difference between the anisotropy strength of the fcc Co and fcc NiFe films; however, the smaller exchange stiffness of the NiFe film defines a smaller NiFe wall width compared to that of the fcc Co film. This exchange stiffness induces a large difference of wall width in the fcc Co spin valve, and this is not favorable for the observation of the mirror domain effect. However, in the case of GaAs spin valves, the exchange stiffness difference is compensated by a difference in anisotropy strength in the bcc (or bcc + hcp) Co films to give comparable domain-wall thickness. We believe the absence of the mirror domain structure in the fcc Co spin valve in the Si system also minimizes the possibility of the interlayer exchange coupling effect being the cause of the mirror domain structure. Both the Si and GaAs systems have the same NiFe/Cu/Co spin-valve structures with a similar Cu spacer layer thickness: if the mirror domain effect were induced by interlayer exchange coupling, such an effect would appear in the measurements of the Si spin-valve system. However, the mirror domain effect is present in all the measurements on the GaAs system but not in the Si system.

In the GaAs/Co(18 Å)/Cu/NiFe sample, the MOKE and GMR measurements show that the field  $H_p$  required to break the pinning of the NiFe domain walls by the Co domain walls is only slightly larger than the coercivity of the NiFe, while the 30 and 40 Å Co spin valves on GaAs systems show a bigger pinning field. Therefore, a carefully chosen investigation system is needed to observe the mirror domain effect, i.e., the wall-wall pinning field must be larger than the NiFe coercivity. A typical value of  $H_p$  was found to be approximately 15 and 60 Oe for the 18-Å-thick and 30-Å-thick Co spin-valve systems on GaAs(100), respectively, providing a

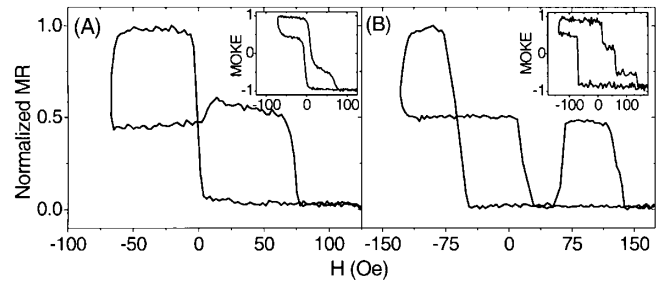


FIG. 5. GMR measurements for (A) Si/Cu/Co(40 Å)/Cu/NiFe and (B) GaAs/Co(30 Å)/Cu/NiFe. The insets show the MOKE results. Mirror domain effects are consistently observed in GaAs samples but not in Si samples. Note that the second step switching is more obvious as the pinning field becomes larger.

direct measurement of the wall-wall interaction energy ( $2\mu_0 M_{\text{NiFe}} H_p$ ) of  $\sim 2.58 \times 10^{-3}$  J/cm<sup>3</sup> and  $\sim 1.03 \times 10^{-2}$  J/cm<sup>3</sup>, respectively.

In conclusion, a long-range domain-wall pinning through a thick spacer layer in NiFe/Cu/Co structures is observed. The pinning has induced an unusual type of mirror domain structure which can account for the sudden drop of GMR during the NiFe reversal. By using the domain-wall stray field from the neighboring Co layer to trap the propagating NiFe domain wall and calibrating the magnitude of the corresponding resistance drop, we clearly demonstrate the presence of the interlayer domain-wall coupling.

- 
- [1] P. Grünberg *et al.*, Phys. Rev. Lett. **57**, 2442 (1986); S. S. P. Parkin *et al.*, Phys. Rev. Lett. **64**, 2304 (1990); J. C. Slonczewski, J. Magn. Magn. Mater. **129**, L123 (1994); P. Bruno, Phys. Rev. B **52**, 411 (1995).
  - [2] M. Stiles, J. Magn. Magn. Mater. **200**, 322 (1999).
  - [3] H. W. Fuller and D. L. Sullivan, J. Appl. Phys. **33**, 1063 (1962).
  - [4] F. Biragnet *et al.*, Phys. Status Solidi **16**, 569 (1966).
  - [5] S. Gider *et al.*, Science **281**, 797 (1998).
  - [6] L. Thomas *et al.*, Phys. Rev. Lett. **84**, 1816 (2000).
  - [7] S. Hope *et al.*, Phys. Rev. B **55**, 11422 (1997).
  - [8] M. T. Johnson *et al.*, Phys. Rev. Lett. **68**, 2688 (1992).
  - [9] W. S. Lew *et al.*, J. Appl. Phys. **87**, 5947 (2000).
  - [10] G. A. Prinz, Phys. Rev. Lett. **54**, 1051 (1985); Y. Z. Wu *et al.*, Phys. Rev. B **57**, 11935 (1998).
  - [11] S. S. P. Parkin *et al.*, Phys. Rev. Lett. **66**, 2152 (1991).
  - [12] H. Yamamoto *et al.*, J. Magn. Magn. Mater. **126**, 437 (1993); Y. Kawawake *et al.*, J. Appl. Phys. **79**, 6231 (1996).
  - [13] S. P. Li *et al.*, Phys. Rev. B **61**, 6871 (2000).
  - [14] H. P. Oepen, J. Magn. Magn. Mater. **93**, 116 (1991).
  - [15] H. W. Fuller and L. R. Lakin, J. Appl. Phys. **34**, 1069 (1963).